PCCP

Investigations on the charge transfer mechanism at donor/acceptor interfaces in quest of descriptors of organic solar cell performance

Journal:	*Physical Chemistry Chemical Physics*
Manuscript ID	CP-ART-02-2018-001253.R1
Article Type:	Paper
Date Submitted by the Author:	02-Apr-2018

Complete List of Authors:	Muraoka, Azusa; Nihon Joshi Daigaku, Department of Mathematical and Physical Sciences; CREST-JST Fujii, Mikiya; The University of Tokyo, Department of Chemical System Engineering; CREST-JST Mishima, Kenji; The University of Tokyo, Department of Chemical System Engineering Matsunaga, Hiroki; Kyoto University, Department of Polymer Chemistry Benten, Hiroaki; Nara Institute of Science and Technology, Graduate School of Materials Science; CREST-JST Ohkita, Hideo; Kyoto University, Department of Polymer Chemistry; CREST-JST Ito, Shinzaburo; Kyoto University, Department of Polymer Chemistry; CREST-JST Yamashita, Koichi; The University of Tokyo; CREST-JST

Investigations on the charge transfer mechanism at donor/acceptor interfaces in quest of descriptors of organic solar cell performance

Azusa Muraoka [1), 3)*], Mikiya Fujii [2), 3)], Kenji Mishima [2)], Hiroki Matsunaga [4)], Hiroaki Benten [3), 5)*], Hideo Ohkita [3), 4)*], Shinzaburo Ito [3), 4)], and Koichi Yamashita [2), 3)*]

1) *Department of Mathematical and Physical Sciences, Japan Women's University, 2-8-1 Mejirodai, Bunkyo-ku, Tokyo 112-8681, Japan*
2) *Department of Chemical System Engineering, Graduate School of Engineering, The University of Tokyo, Tokyo 113-8656, Japan*
3) *CREST-JST, 7 Gobancho, Chiyoda-ku, Tokyo 102-0076, Japan*
4) *Department of Polymer Chemistry, Graduate School of Engineering, Kyoto University, Katsura, Nishikyo, Kyoto 615-8510, Japan*
5) *Graduate School of Materials Science, Nara Institute of Science and Technology, Takayama-cho, Ikoma, Nara 630-0192, Japan*

* Corresponding authors:
muraokaa@fc.jwu.ac.jp, benten@ms.naist.jp, ohkita@photo.polym.kyoto-u.ac.jp, yamasita@chemsys.t.u-tokyo.ac.jp

Abstract

We theoretically and experimentally investigate the mechanisms of charge separation processes of organic thin-film solar cells. PTB7, PTB1 and PTBF2 are chosen as donors and $PC_{71}BM$ as acceptors, considering the effective charge generation depends on the difference between the materials combinations. Experimental results

of transient absorption spectroscopy show that "hot" process is a key step for determining external quantum efficiency (EQE) in these systems. From the quantum chemistry calculations, it turns out that EQE tends to increase as transferred charge, charge transfer distance, and variation of dipole moments between the ground and excited states of the donor/acceptor complexes increase, which indicates that these physical quantities are a good "descriptor" to assess the donor–acceptor charge transfer quality contributing to the solar cell performance. We propose that designing D/A interfaces having large values of the charge transfer distance and variation of dipole moments of the donor/acceptor complexes is a prerequisite for developing the high-efficiency polymer/PCBM solar cells.

I. Introduction

It is well known that efficient exciton dissociation into separated electron and hole states (free carriers) leads to increased photocurrent, thus enhancing power conversion efficiencies (PCEs) in organic solar cells [1]. It is increasingly recognized that one of the puzzling problems to be clarified in the mechanism of organic thin-film solar cells is whether the charge separation (CS) of an electron and a hole is a "hot" or a "cool" process. An electro-optical pump-push experiment [2] has shown that in efficient photoconversion systems, the hot-state charge delocalization is more dominant than the energy-gradient-driven intermolecular hopping for CS. In a similar way, using a Green's function approach to calculate the generation rates of charge transfer (CT) states, it was found that exciton dissociation led to partially separated charges, the final states of which are "hot" CT states, with electron and the hole being situated far from the interface [3].

This challenging issue has been addressed in terms of the lowest CT state (CT_1) [4] and in terms of long-range and energetically higher CT states at the donor/acceptor (D/A) interface [5]. In the former case, the internal quantum efficiency (IQE) was found to be essentially independent on whether states higher than that of CT_1 are excited or not. In addition, that study found that CT_1 which is weakly bound and has an energy close to that of the CS state generates charge at high efficiency (>90%) at all photon energies equal to and larger than the energy of CT_1. In contrast, in the latter case, it was confirmed that the energetically higher CT states ("hot" CT excitons) have several advantages over the short-range CT states. That is, "hot" CT excitons are usually spatially delocalized and therefore are not easily trapped by the attractive Coulomb force between an electron and a hole. In addition, they have an external

quantum efficiency (EQE) that is much higher than that of the low-lying CT states that are accessible via the internal conversion process [4].

Recent studies have focused on the importance of the variation in dipole moments for efficient charge generation [6–9]. Yu *et al.* have suggested that the variation in dipole moments in *intra*molecular charge transfer in the donor molecule (denoted as $\Delta\mu_D$) is crucial in controlling PCE [6,7]. They showed that an internal dipole moment along the polymer chain is critical in maintaining the pseudo-charge-transfer characteristics comparing the PCEs of PBB3 and PTB7 copolymers, which have smaller and larger dipole moments, respectively; the latter have larger PCE and J_{SC} compared with the former. On the other hand, we have confirmed by experiments and quantum chemistry calculations on the photophysical and electrochemical properties of complexes of diketopyrrolopyrrole-based donors and a PCBM acceptor that the variation in dipole moments between the ground and excited states of the D/A complexes ($\Delta\mu_{D/A}$) rather than $\Delta\mu_D$ plays a crucial role in determining solar cell efficiency [8,9].

Despite the numerous conjectures on the most probable CS mechanisms proposed so far, a satisfactory consensus has not yet been obtained. Therefore, to investigate the matter further, it is desirable to identify some likely descriptors to quantify CS efficiency. In this paper, we propose to use the transferred charge (denoted as ΔQ), the charge transfer distance (denoted as d_{CT}), and $\Delta\mu_{D/A}$ as a promising descriptor for the estimation CS efficiency [10,11]. ΔQ, $d_{CT,}$ and $\Delta\mu_{D/A}$ are easily calculable using the widespread density functional theory (DFT) and time-dependent density functional theory (TD-DFT), and we can numerically ascertain the correlation between ΔQ, $d_{CT,}$ $\Delta\mu_{D/A}$ and CS efficiency. Furthermore, it would be useful to design

highly efficient organic solar cell materials without resorting to experiment.

This paper has three principal aims: (1) to experimentally determine whether the CS process takes place by a "hot" or "cool" process in the PTB7/$PC_{71}BM$, and PTB1/$PC_{71}BM$, PTBF2/$PC_{71}BM$ systems; (2) to numerically examine whether direct optical generation of CT states takes place in the CS process of these systems; and (3) to show that d_{CT} and $\Delta\mu_{D/A}$ are promising "descriptors" for the quantification of CS efficiency of organic solar cells.

II. Methods

Theoretical

The quantum chemistry calculations of absorption spectra of D/A complexes were performed using the GAUSSIAN 09 program package [12]. The molecular structures were optimized using the DFT calculations at the ωB97XD/6-31G(d) level of theory. For D/A complexes, we consider PTB7, PTB1 and PTBF2 as the donor molecule and $PC_{71}BM$ as the acceptor molecule (see Fig. 1). The hydrocarbon side chains of the donor molecules are replaced with the methyl group. The absorption spectra of D/A systems were calculated by TD-DFT at the CAM-B3LYP/6-31G(d) level of theory [13,14].

The quantities, ΔQ, $d_{CT,}$ and $\Delta\mu_{D/A,}$ were estimated using the quantum chemistry calculation results according to [10,11]. The details are recapitulated in Section 1 of Supporting Information (SI). The calculations were performed using the code available at no cost on the website [15].

Experimental

***Materials*:**

Polymer donors, poly[[4,8-bis[(2-ethylhexyl)oxy]benzo[1,2-*b*:4,5-*b*']dithiophene-2,6-diyl][3-fluoro-2-[(2-ethylhexyl)carbonyl]thieno[3,4-*b*]thiophenediyl]] (PTB7) (M_w = 122000 g mol^{-1}, M_w/M_n = 2.4) and poly[[4,8-bis(octyloxy)benzo[1,2-*b*:4,5-*b*']dithiophene-2,6-diyl][2-[(dodecyloxy)carbonyl]thieno[3,4-*b*]thiophenediyl]] (PTB1, M_w = 83000 g mol^{-1}, M_w/M_n = 3.7) were obtained from 1-Material Inc. and Luminescence Technology Crop., respectively, and used as received. An acceptor, [6,6]-phenyl-C_{71}-butyric acid methyl ester ($PC_{71}BM$, nanom spectra E112) was obtained from Frontier Carbon, and used as received.

***Sample preparation*:**

Neat films of PTB7 and PTB1 were prepared on sapphire substrates by spin-coating from chlorobenzene : 1,8-diiodooctane (97 : 3 weight ratio) solutions. Blend films of PTB7/$PC_{71}BM$ and PTB1/$PC_{71}BM$ were prepared on sapphire substrates by spin-coating from chlorobenzene : 1,8-diiodooctane (97 : 3 weight ratio) solutions of polymer and $PC_{71}BM$. The polymer : $PC_{71}BM$ weight ratio in the solution was 1 : 1.5.

***Transient absorption (TA) measurements*:**

TA data were collected using a femtosecond pump and probe TA spectroscopy system, which consists of a TA spectrometer (Ultrafast Systems, Helios) and a regenerative amplified Ti:sapphire laser (Spectra-Physics, Hurricane) [16]. The temperature dependence of the TA signals was obtained from 77 to 294 K in a vacuum using a cryostat (Optistat DN-V, Oxford Instruments) fitted with a temperature control unit (ITC503S, Oxford Instruments). The excitation of the polymer/$PC_{71}BM$ blend

films was conducted at wavelength of 680 nm or 740 nm to excite polymer mainly.

III. Results and Discussion

***Absorption and TA spectra*:**

Absorption spectra of the PTB7/$PC_{71}BM$ and PTB1/$PC_{71}BM$ blend films used for the TA measurements are shown in Fig. 2.

Figures 3a and 3b show the TA spectra of the PTB7 and PTB1 neat films, measured at 1 and 1000 ps after excitation at 680 nm. Both polymer donors showed negative TA spectrum below 750 nm, corresponding to the transient ground-state bleach, which was determined by comparing the data with the steady-state absorption spectrum (Fig. 2). The broad positive TA signal that ranges at wavelengths longer than 750 nm and peaks at around 1350 nm is assigned to singlet excitons of polymer donors. After 1000 ps, the TA signals distinguished. Figures 3c and 3d show the TA spectra of the PTB7/$PC_{71}BM$ and PTB1/$PC_{71}BM$ blend films, measured at 1, 100, and 1000 ps after excitation at 680 nm. The spectral features at wavelengths longer than 750 nm are clearly different from the spectra of the polymer singlet excitons, even 1 ps after excitation and the TA signal still remains at time domains longer than 1000 ps. The spectral features of the new TA signal is very similar to those of polymer hole polarons, which was obtained by doping the polymer neat films with iodine (Fig. 4). We therefore ascribed the TA signals with peak at 1100 nm in Figs. 3c and 3d to polymer hole polarons generated at the polymer/$PC_{71}BM$ heterojunctions.

***Charge Generation*:**

As shown in Fig. 3, for the PTB7/$PC_{71}BM$ blend film, no TA signal from PTB7 singlet excitons is observed even 1 ps after excitation, indicating that charge generation

is completed at <1 ps. For the PTB1/$PC_{71}BM$ blend film, the TA signal from both PTB1 singlet excitons (at 1350 nm) and hole polarons (at 1100 nm) are observed at 1 ps after excitation, while the TA signal from singlet excitons rapidly disappears within a few tens of ps. To analyze the charge generation dynamics in the PTB1/$PC_{71}BM$ blend film, we resolved the TA spectra into PTB1 singlet exciton and charged species by spectral simulation. Here, the TA spectrum at 1000 ps after excitation was used as a spectrum of the charged species. Figure 5 shows time evolution of the PTB1 hole polarons at 1100 nm. The 60% of PTB1 hole polarons were promptly generated at <1 ps, and the subsequent delayed charge generation ends at 50 ps. The immediate charge generation which completes at <1 ps demonstrate that charge transfer (exciton dissociation) occurs so quickly in the both PTB7/$PC_{71}BM$ and PTB1/$PC_{71}BM$ blend films as has been reported for other polymer/PCBM blend films.[17] The delayed charge generation observed in PTB1/$PC_{71}BM$ blend film is attributed to a diffusion controlled process, which represents the time required for the polymer singlet exciton to diffuse to the polymer/$PC_{71}BM$ heterojunctions.

***Charge Recombination*:**

Figure 6 shows the decay dynamics of the polymer hole polarons at 1100 nm. The ΔOD was normalized; the maximum peak intensities at 1 ps for PTB7/$PC_{71}BM$ blend and at 50 ps for PTB1/$PC_{71}BM$ were set to 1. For PTB7/$PC_{71}BM$ blend film, the ΔOD did not decay within a time domain from 1 to 1500 ps. For PTB1/$PC_{71}BM$ blend film, on the other hand, the time evolution of ΔOD on a time domain of >50 ps was represented by sum of a decay component with a lifetime of several hundreds of ps and a non-decaying component: $\Delta OD = A\exp(-t/\tau) + B$. Moreover, the decay lifetime was independent of the excitation intensity at laser intensities below 10 μJ cm^{-2}, suggesting

monomolecular recombination. The non-decaying component observed for both polymer/$PC_{71}BM$ blend films was ascribed to the spatially separated free carriers that survive against the recombination. In contrast, the decay component was ascribed to geminate charge recombination. On the basis of these assignments, free carrier generation efficiency (η) was defined from the fraction of the non-decaying charges in the whole generated charges. The value of η was estimated to 100% for PTB7/$PC_{71}BM$ and 80% for PTB1/$PC_{71}BM$ blend film, which was summarized in Table 1.

The EQE observed experimentally differed between all the D/A combinations (Table 2) at 65–70%, 55–60%, and ~45% for the PTB7/$PC_{71}BM$, PTB1/$PC_{71}BM$, and PTBF2/$PC_{71}BM$ systems, respectively. This implies that the difference of EQE of this kind is one of the factors governing J_{SC}. To clarify the origin of this difference, recalling that the value of the free carrier generation efficiency (η) was 100% in the PTB7/$PC_{71}BM$ system and 80% in the PTB1/$PC_{71}BM$ system, respectively, which is quantitatively consistent with the EQE and J_{SC} superior observed in the PTB7/$PC_{71}BM$ system [18].

In addition, we examined whether the free carrier generation process is temperature-independent "hot" process and temperature-dependent "cool" process by measuring the temperature dependence of η. Then, the η values were confirmed from Fig. 5 to be temperature independent between 77 and 294 K, indicating that exciton dissociation into spatially separated free hole and electron is temperature independent process, that is, the exciton dissociation surviving monomolecular recombination should not be a thermally activation process on uphill energy surface from the lowest CT state. Namely, the main route of the free carrier generation is the "hot" process in both

PTB7/$PC_{71}BM$ and PTB1/$PC_{71}BM$ systems. In other words, the primary factor of providing the PTB7/$PC_{71}BM$ system with the better solar cell performance is the efficient free carrier generation via the "hot" process in the PTB7/$PC_{71}BM$ system.

***Theoretical Descriptors*:**

To clarify the reason behind the efficiency of free carrier generation, we investigated the charge transfer mechanisms at the PTB/$PC_{71}BM$ interface using quantum chemistry calculations. In Fig. 7, the stabilization energies (in hartree) are plotted versus the intermolecular distance between the donor and acceptor molecules (Å) and the most stable intermolecular structures of the PTB7/$PC_{71}BM$ (Fig. 7a), the PTB1/$PC_{71}BM$ (Fig. 7b), and the PTBF2/$PC_{71}BM$ (Fig. 7c) systems, when $PC_{71}BM$ is placed facedown on the donor molecule. It can be seen that the stabilization energies are ≈ 0.33 eV, ≈ 0.37 eV and ≈ 0.43 eV for the PTB7/$PC_{71}BM$, PTB1/$PC_{71}BM$, and PTBF2/$PC_{71}BM$ systems, respectively. The intermolecular energy minimum is attained at the intermolecular distance of ≈ 3.5 Å in Fig. 7a, ≈ 3.2 Å in Fig. 7b and ≈ 3.0 Å in Fig. 7c. The stabilization energies and the intermolecular energy minima are reasonably correlated, that is, as the latter decreases the former increases. For the intermolecular distances between the fullerenes and π-functional donors, Borges et al. [19] estimated 3.19 Å for /$PC_{60}BM$ at the PBE(D)/SV-SVP level and Liu and Trois [20] estimated 3.5 Å for poly(3-methylthienylene)/$PC_{60}BM$ at the B3LYP/6-31G* level.

Figure 8 shows the numerically calculated absorption spectra of the representative D/A systems optimized in Fig. 7 (three-molecules donor/one-molecule acceptor: PTB7/$PC_{71}BM$, PTB1/$PC_{71}BM$, and PTBF2/$PC_{71}BM$). We have assumed here that the donors are trimer because trimer are sufficient for realistically perform quantum chemistry calculations as shown in Fig. S1 (ESI). The absorption spectra

seem to be almost identical in all D/A combinations and the most intense components of the absorption spectra include a D/A character. The latter fact indicates that an efficient charge transfer may take place in all D/A combinations. In addition, it is noted that many absorption peaks also have a D/A character at wavelengths other than that of the absorption peak. Overall, the absorption spectra show almost the same tendency in all of the D/A systems shown in Fig. 8. Figure 8a and the experimentally observed spectrum [18] do not agree for the reasons explained in Section 2 of the SI. From Table 2, it can be seen that the experimentally observed EQE is quite different between all D/A combinations. Therefore, comparing Fig. 8 and Table 2, it can be concluded that there is no correlation between the absorption spectra of the D/A complexes and solar cell performance. Table 3 summarizes the percentage of D/A and D/D transitions at the strongest absorption peak. The molecular orbitals involved in the absorption transitions are shown in Figs. 9–11 for the PTB7/$PC_{71}BM$, PTB1/$PC_{71}BM$, and PTBF2/$PC_{71}BM$ systems, respectively.

From Table 3, the direct D/A absorption transitions to the more highly excited CT configurations can be found for the PTB7/$PC_{71}BM$ system (3% for HOMO−2 → LUMO+1 transition, 3% for HOMO−1 → LUMO+4 transition, and 10% for HOMO−1 → LUMO+5 transition, i.e., 16% in total) while there are less direct D/A absorption transitions to the more highly excited CT configurations for the PTB1/$PC_{71}BM$ system (3% for HOMO−2 → LUMO transition, 5% for HOMO−2 → LUMO+1 transition, 7% for HOMO → LUMO+1 transition, i.e., 15% in total). The percentage is even smaller for the PTBF2/$PC_{71}BM$ system (7% for HOMO−1 → LUMO+4 transition and 3% for HOMO → LUMO+2 transition, i.e., 10% in total). This difference results in the free carrier generation via “hot” process more probable in the PTB7/$PC_{71}BM$ system

because the direct D/A absorption transition to highly excited states is one of the direct consequences of the dense density of states (DOS's) of the spatially extended highly excited CT states [5].

Table 2 shows the amount of transferred charge (ΔQ), the charge transfer distance (d_{CT}), and the variation of the dipole moments between the ground and excited states of the D/A complexes ($\Delta\mu_{D/A}$) calculated according to [9,10] in the PTB7/$PC_{71}BM$, PTB1/$PC_{71}BM$, and PTBF2/$PC_{71}BM$ systems. It can be seen that the EQE and J_{SC} becomes larger as ΔQ, d_{CT}, and $\Delta\mu_{D/A}$ increase (in particular, the PTB7/$PC_{71}BM$ system is better than the PTBF2/$PC_{71}BM$ system). This agrees with the observation from [7,8] that $\Delta\mu_{D/A}$ increases as the EQE increases. This comparative examination indeed indicates that ΔQ, $d_{CT,}$ and $\Delta\mu_{D/A}$ rather than $\Delta\mu_D$ are a good "descriptor" for assessing the donor quality contributing to solar cell performance.

From these results, ΔQ, $d_{CT,}$ and $\Delta\mu_{D/A}$ (but not necessarily $\Delta\mu_D$) can be seen as the key factors for controlling EQE; thus, the design of D/A interfaces with large values of ΔQ, d_{CT}, and $\Delta\mu_{D/A}$ is a prerequisite for developing high-efficiency polymer/PCBM solar cells.

IV. Conclusion

We have experimentally and theoretically investigated the mechanism of CS processes of the PTB7/$PC_{71}BM$, PTB1/$PC_{71}BM$, and PTBF2/$PC_{71}BM$ systems in detail in quest for "descriptors" governing organic solar cell efficiency. We summarize our findings as follows.

First, from the TA spectroscopy, it was found that the difference in the EQEs for the polymer/PCBM systems is well correlated with the difference in the free carrier

generation efficiencies. Second, from the comparison between the numerical absorption spectra and the experimentally observed EQE, we found that there is no correlation between the absorption characteristics of D/A complexes and solar cell performance. Third, because the transferred charge, the charge transfer distance, and the variation of dipole moments prominently increase with increasing value of EQE, these three physical quantities were shown to be good descriptors for assessing the D/A quality contributing to solar cell performance. It should be stressed that the variation in dipole moments addressed here is that between donors and acceptors, and not between donors or between acceptors themselves.

In this paper, we only considered the minimal three-donors/one-acceptor systems. In actual BHJ organic solar cells, a number of complexities inherent in BHJ organic solar cells have to be taken into account, e.g., the relative dielectric constants, morphology, crystallinity, charge mobility, and the intermolecular stacking of the constituent materials. Therefore, to gain a deeper insight into the real exciton dissociation process, a large-scale molecular simulation mimicking actual BHJ organic solar cells will be needed in the future.

Acknowledgments

This work was supported by CREST-JST (No. JPMJCR12C4) and by MEXT as “Priority Issue on Post-K computer” (Development of new fundamental technologies for high-efficiency energy creation, conversion/storage and use). The computations were performed using the Research Center for Computational Science, Okazaki, Japan and the facilities of the Supercomputer Center, the Institute for Solid State Physics, the University of Tokyo, Japan.

References

[1] T. M. Clarke, A. Ballantyne, S. Shoaee, Y. W. Soon, W. Duffy, M. Heeney, I. McCulloch, J. Nelson and J. R. Durrant, *Adv. Mater*., 2010, **22,** 5287.

[2] A. A. Bakulin, A. Rao, V. G. Pavelyev, P. H. M. van Loosdrecht, M. S. Pshenichnikov, D. Niedzialek, J. Cornil, D. Beljonne and R. H. Friend, *Science*, 2012, **335,** 1340.

[3] H. V. Vazquez and A. Troisi, *Phys. Rev. B*, 2013, **88,** 205304.

[4] K. Vandewal, S. Albrecht, E. T. Hoke, K. R. Graham, J. Widmer, J. D. Douglas, M. Schubert, W. R. Mateker, J. T. Bloking, G. F. Burkhard, A. Sellinger. J. M. J. Fréchet, A. Amassian, M. K. Riede, M. D. McGehee, D. Neher and A. Salleo, *Nat. Mater.*, 2014, **13,** 63.

[5] H. Ma and A. Troisi, *Adv. Mater.*, 2014, **26,** 6163.

[6] B. Carsten, J. M. Szarko, H. J. Son, W. Wang, L. Lu, F,. He, B. S. Rolczynski, S. J. Lou, L. X. Chen and L. Yu, *J. Am. Chem. Soc.,* 2011, **133,** 20468.

[7] J. M. Szarko, B. S. Rolczynski, S. J. Lou, T. Xu, J. Stzalka, T. J. Marks, L. Yu and L. X. Chen, *Adv. Func. Mater.,* 2014, **24,** 10.

[8] M. Fujii, W. Shin, T. Yasuda and K. Yamashita, *Phys. Chem. Chem. Phys.*, 2016, **18,** 9514.

[9] S. Koda, M. Fujii, S. Hatamiya and K. Yamashita, *Theor. Chem. Acc.,* 2016, **135,** 115.

[10] T. L. Bahers, C. Adamo and I. Ciofini, *J. Chem. Theory Comput.*, 2011, **7,** 2498.

[11] D. Jacquemin, T. L. Bahers, C. Adamo and I. Ciofini, *Phys. Chem. Chem. Phys.,* 2012, **16,** 5383.

[12] M. J. Frisch, *et al*., *GAUSSIAN 09*, Gaussian, Inc., Wallingford, CT, 2009.

[13] A. Dreuw and M. Head-Gordon, *Chem. Rev.*, 2005, **105,** 4009.

[14] T. Yanai, D. P. Tew and N. C. Handy, *Chem. Phys. Lett.*, 2004, **393,** 51.

[15] http://www.sciences.univ-nantes.fr/CEISAM/erc/marches/

[16] D. Mori, H. Benten, H. Ohkita and S. Ito, *Adv. Energy. Mater.*, 2015, **5,** 1500304.

[17] J. Guo, H. Ohkita, H. Benten and S. Ito, *J. Am. Chem. Soc.,* 2010, **132,** 6154.

[18] Y. Liang, Z. Xu, J. Xia, S.- T. Tsai, Y. Wu, G. Li, C. Ray and L. Yu, *Adv. Mater.,* 2010, **22,** E135.

[19] I. Borges, Jr., A. J. A. Aquino, A. Köhn, R. Nieman, W. L. Hase, L. X. Chen and H. Lischka, *J. Am. Chem. Soc.*, 2013, **135**, 18252.

[20] T. Liu and A. Trois, *J. Phys. Chem. C*, 2011, **115**, 2406.

Figure captions

Fig. 1. Chemical structures of (a) PTB7, (b) PTB1, (c) PTBF2, and (d) $PC_{71}BM$.

Fig. 2. Absorption spectra of the PTB7/$PC_{71}BM$ (black) and PTB1/$PC_{71}BM$ (red) blend films. The polymer: $PC_{71}BM$ weight ratio is 1:1.5.

Fig. 3. TA spectra for the (a) PTB7 neat, (b) PTB1 neat, (c) PTB7/$PC_{71}BM$ blend, and (d) PTB1/$PC_{71}BM$ blend films, measured at delay times of 1 ps (black lines), 10 ps (green lines), 100 ps (blue lines), and 1000 ps (red lines) after excitation. The excitation wavelength was 680 nm and the intensity was 5 μJ cm^{-2} (polymer neat films), 1.25 μJ cm^{-2} (PTB7/ $PC_{71}BM$), and 2.5 μJ cm^{-2} (PTB1/ $PC_{71}BM$). TA spectra of the polymer neat films and polymer/$PC_{71}BM$ blend films were measured at 294 K and 77 K, respectively.

Fig. 4. Absorption spectra of the (a) PTB7 and (b) PTB1 hole poralons. These spectra were obtained by subtracting the absorption spectrum of polymer neat film before doping from that after doping with iodine.

Fig. 5. Time evolution of PTB1 hole polarons at 1100 nm in the PTB1/$PC_{71}BM$ blend film.

Fig. 6. Time evolution of polymer hole polarons at 1100 nm in (a) PTB7/$PC_{71}BM$ and (b) PTB1/$PC_{71}BM$ blend films measured at 77 K (black lines) and 294 K (red lines). The excitation intensity was 0.8 – 1.25 μJ cm^{-2}.

Fig. 7. Stabilization energies (hartree) versus intermolecular distance (Å) and the most stable intermolecular structures of (a) PTB7/$PC_{71}BM$, (b) PTB1/$PC_{71}BM$, and (c) PTBF2/$PC_{71}BM$ systems when $PC_{71}BM$ is placed facedown on the donor molecule.

Fig. 8. Numerically calculated absorption spectra of three-molecules donor/one-molecule acceptor systems: (a) PTB7/$PC_{71}BM$, (b) PTB1/$PC_{71}BM$, and (c) PTBF2/$PC_{71}BM$). The red bars include a donor/acceptor character as well as donor/donor, acceptor/acceptor, and acceptor/donor characters, whereas those without the donor/acceptor character are indicated by blue bars.

Fig. 9. Molecular orbitals of the PTB7/$PC_{71}BM$ system.

Fig. 10. Molecular orbitals of the PTB1/$PC_{71}BM$ system.

Fig. 11. Molecular orbitals of the PTBF2/$PC_{71}BM$ system.

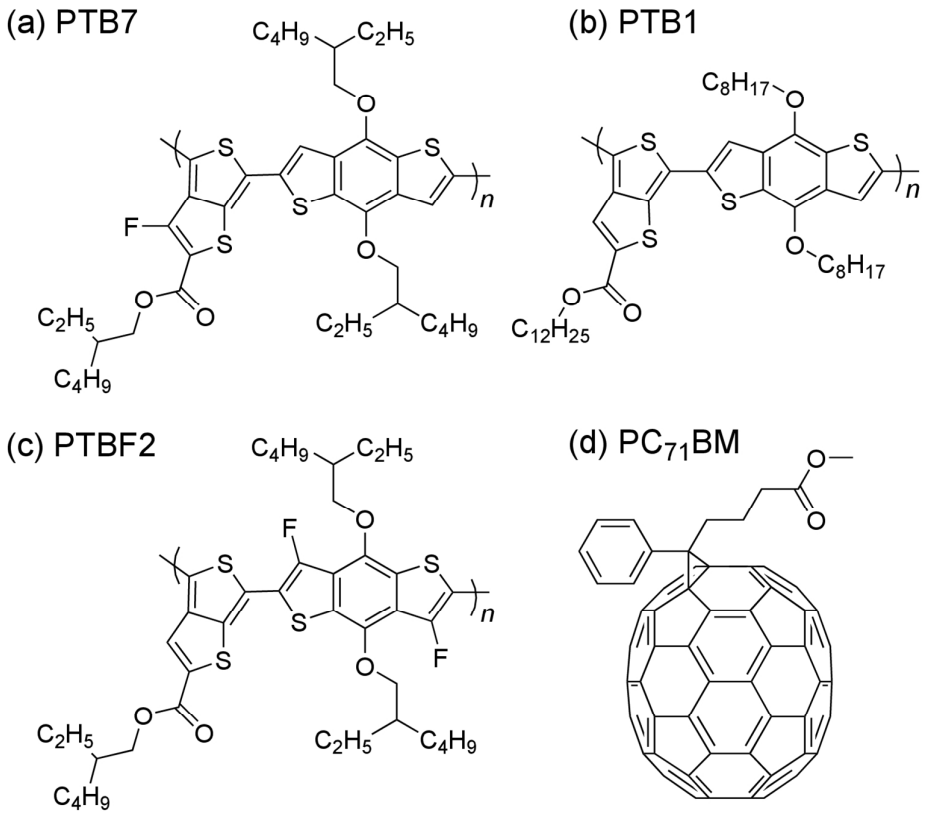

Figure 1 Muraoka *et.al*

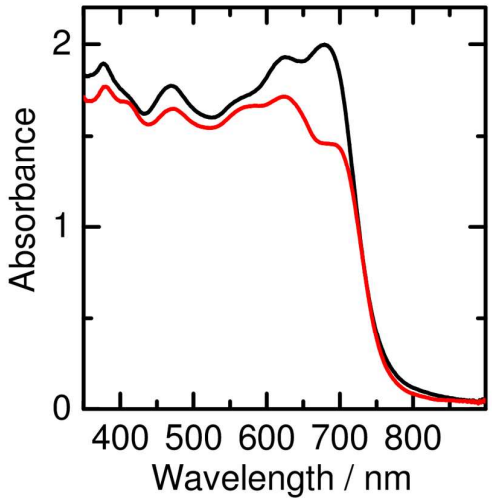

Figure 2 Muraoka *et.al*

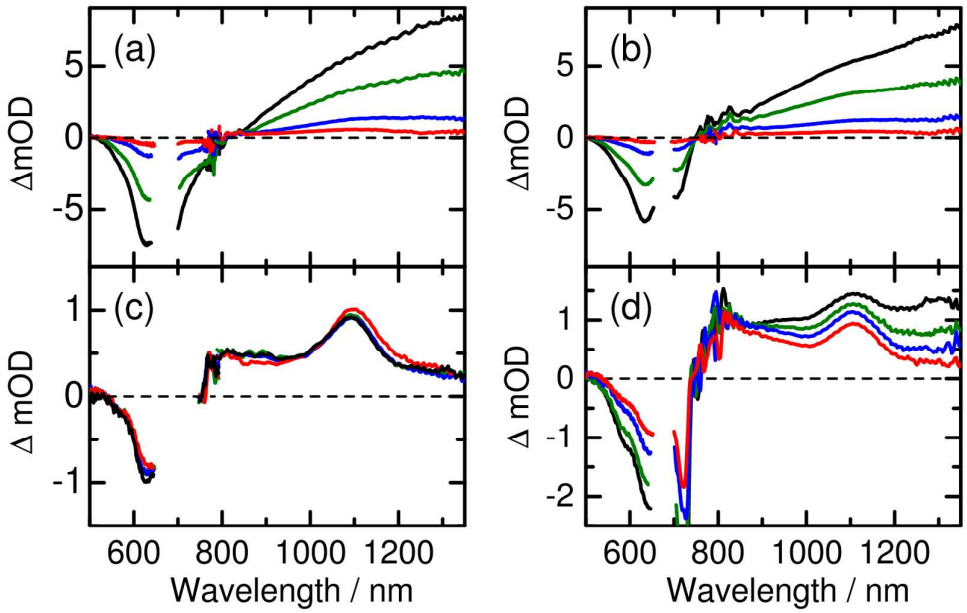

Figure 3 Muraoka *et.al*

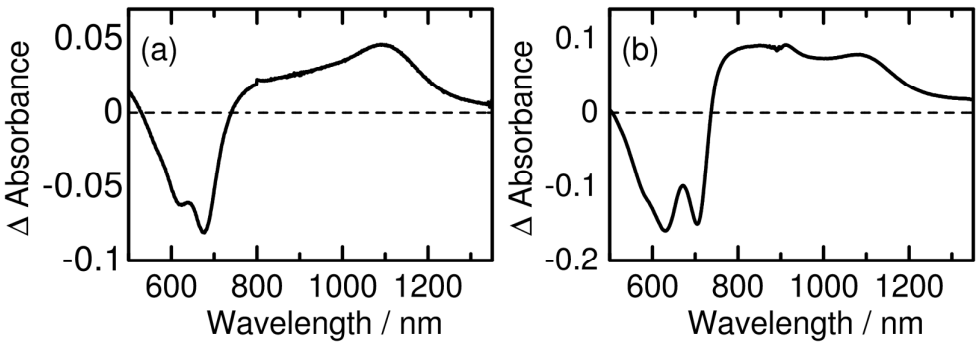

Figure 4 Muraoka *et.al*

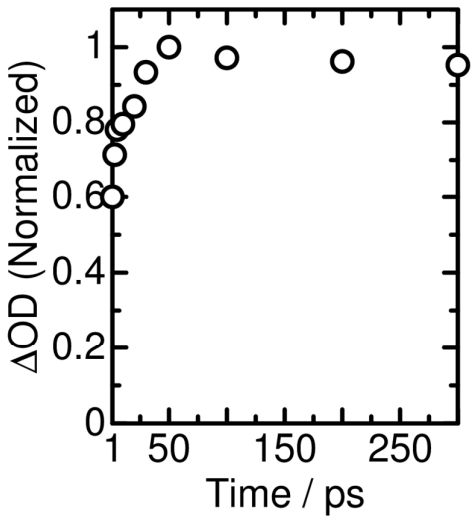

Figure 5 Muraoka *et.al*

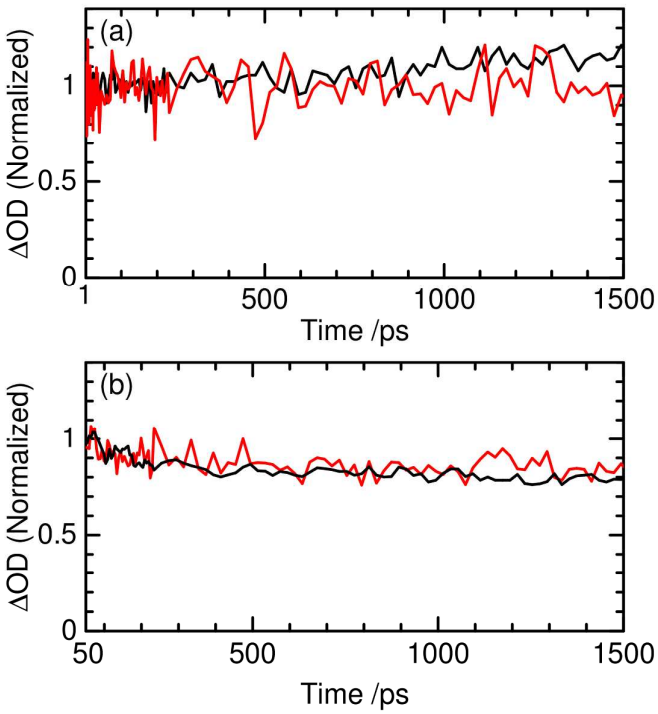

Figure 6 Muraoka *et.al*

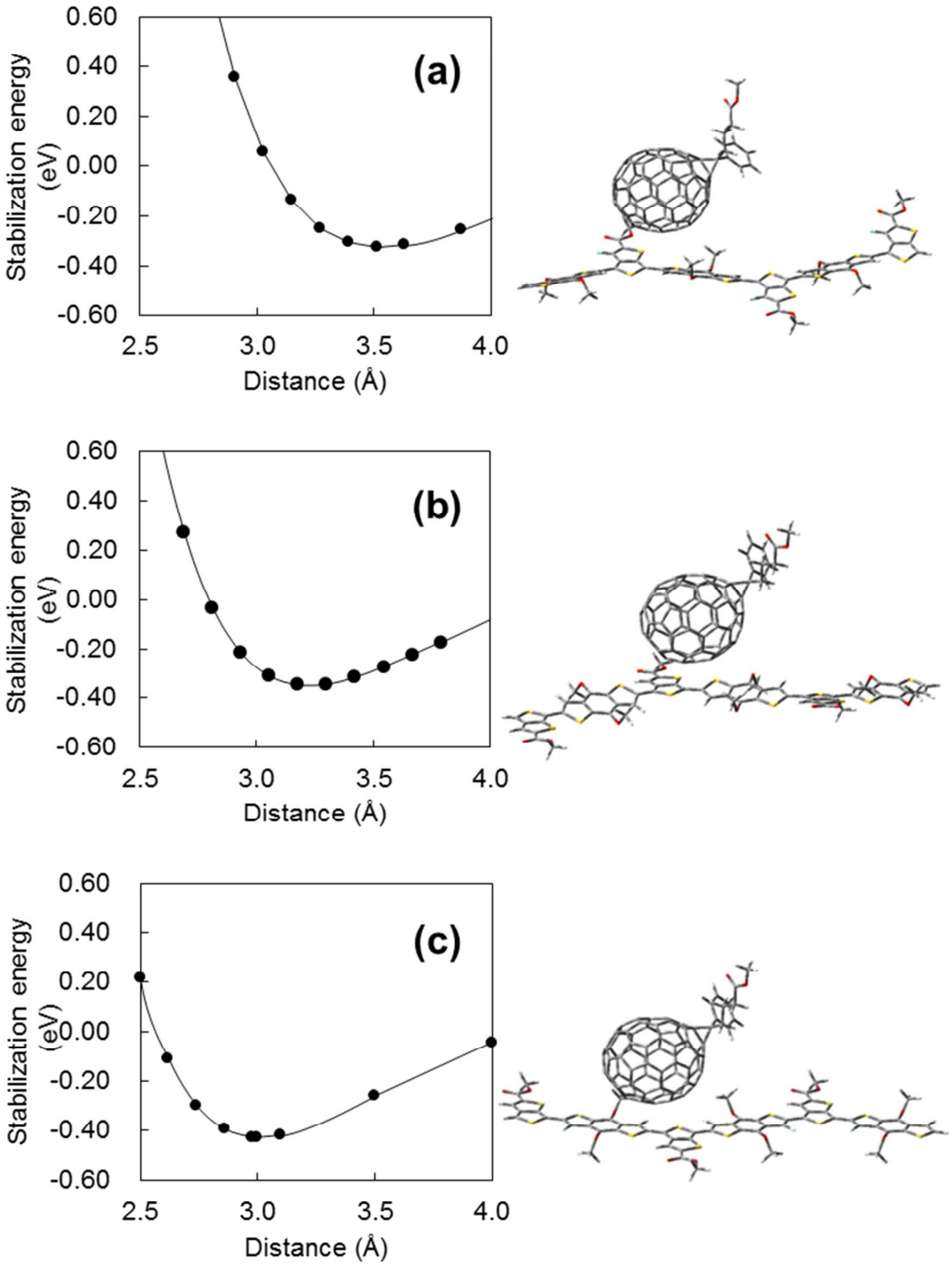

Figure 7 Muraoka *et.al*

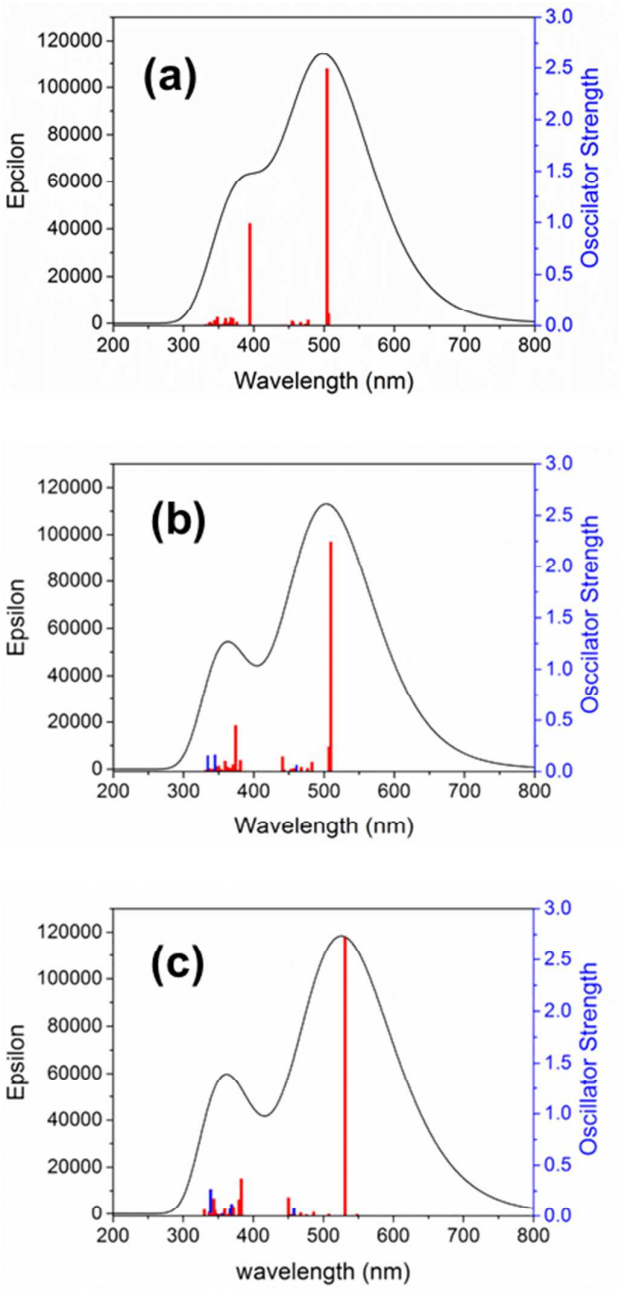

Figure 8 Muraoka *et.al*

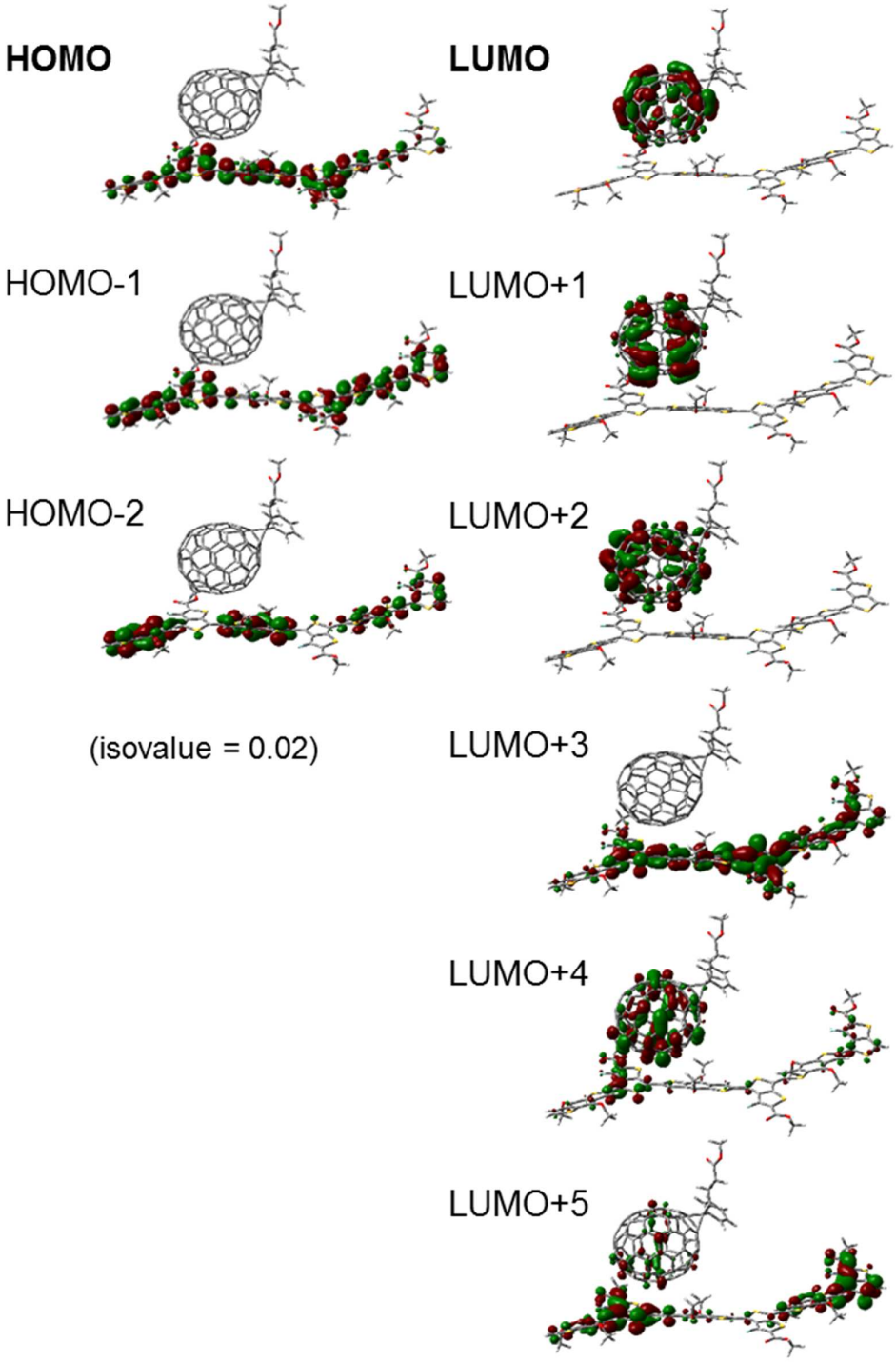

Figure 9 Muraoka *et.al*

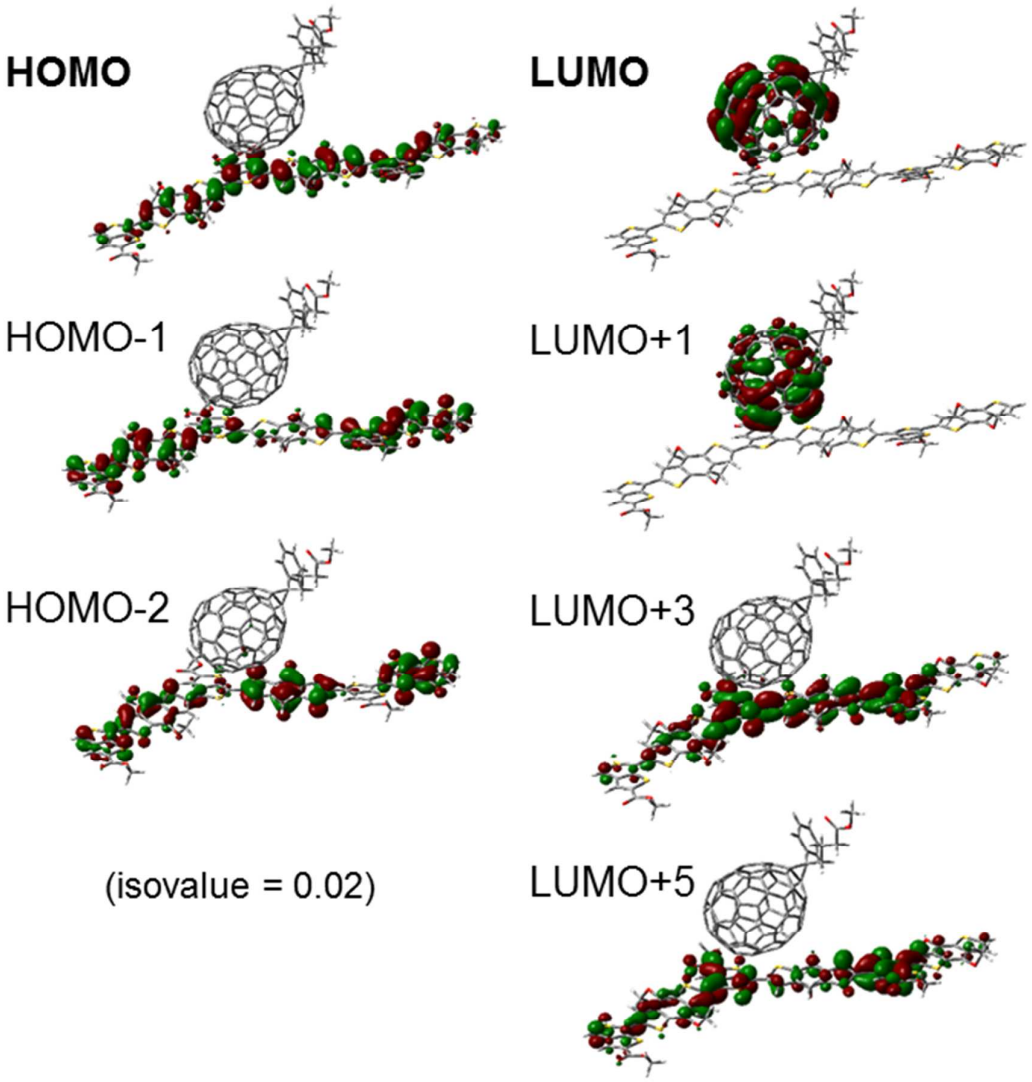

Figure 10 Muraoka *et.al*

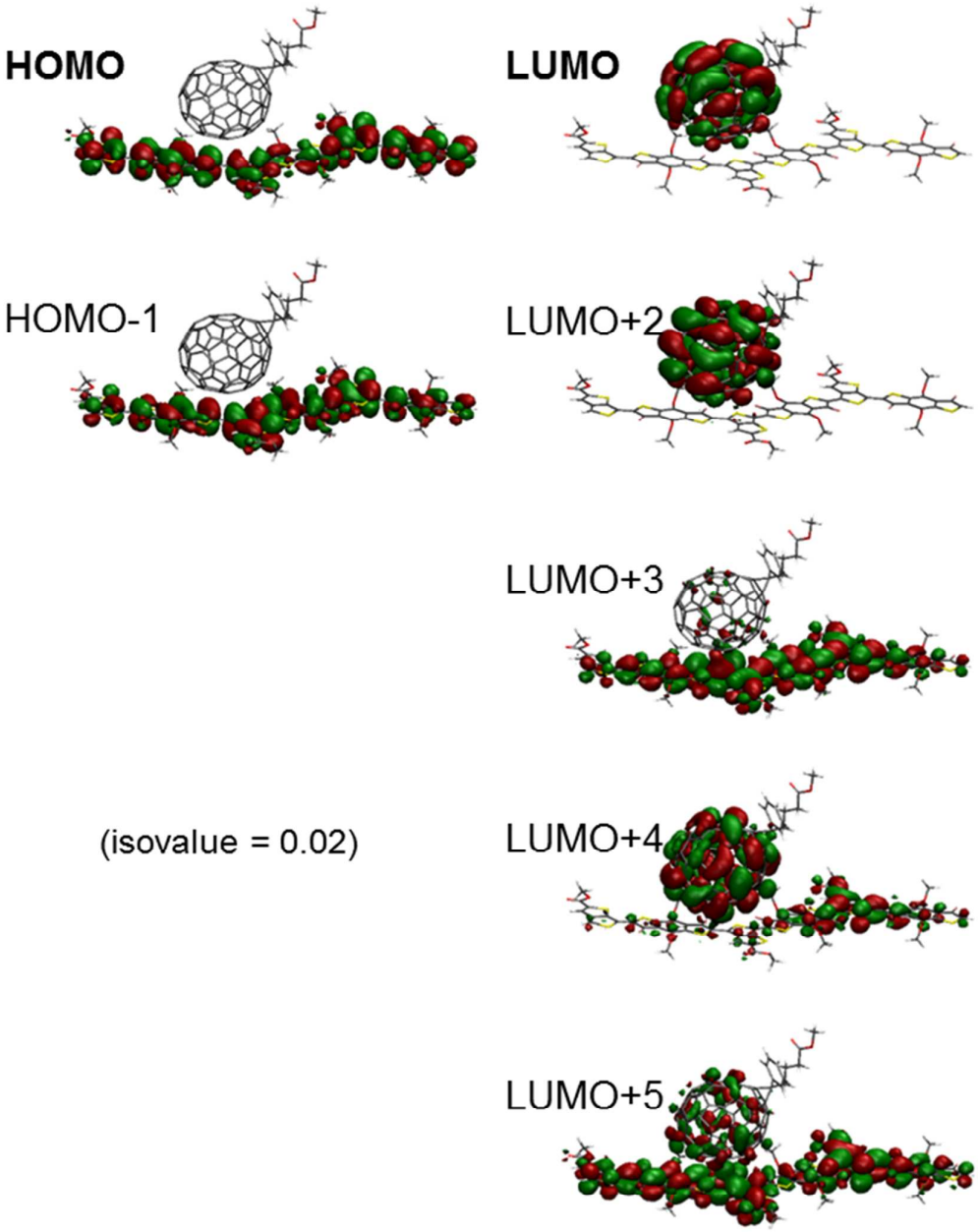

Figure 11 Muraoka *et.al*

Table 1. Experimental result for the free carrier generation efficiency (η).

System	PTB7/$PC_{71}BM$	PTB1/$PC_{71}BM$
η (%)[a]	100	80

[a] The value of η was defined from the fraction of the non-decaying charges in the whole generated charges (Supporting Information).

Table 2. Comparison between J_{SC} and EQE measured experimentally and the amount of transferred charge (ΔQ), charge transfer distance (d_{CT}), and variation of the dipole moments between the ground and excited states of the D/A complexes ($\Delta\mu_{D/A}$) in the PTB7/$PC_{71}BM$, PTB1/$PC_{71}BM$, and PTBF2/$PC_{71}BM$ systems.

System	PTB7/$PC_{71}BM$	PTB1/$PC_{71}BM$	PTBF2/$PC_{71}BM$
J_{SC} (mA cm^{-2})	14.5	14.1	11.1
EQE (%)[a]	65–70	55–60	~45
ΔQ	0.552	0.497	0.467
d_{CT} (Å)	1.020	0.418	0.202
$\Delta\mu_{D/A}$ (Debye)	2.707	0.999	0.453

[a] EQEs at absorption wavelengths of the polymer donors from 600 to 675 nm.

Table 3. Percentages of donor/acceptor and donor/donor transitions at the strongest absorption peak for the PTB7/$PC_{71}BM$, PTB1/$PC_{71}BM$, and PTBF2/$PC_{71}BM$ systems.

System	Absorption transition	Transition type	Percentage (%)
PTB7/$PC_{71}BM$	HOMO−2 → LUMO+1	D → A	3
	HOMO−1 → LUMO+4	D → A	3
	HOMO−1 → LUMO+5	D → A	10
	HOMO → LUMO+3	D → D	84
PTB1/$PC_{71}BM$	HOMO−2 → LUMO	D → A	3
	HOMO−2 → LUMO+1	D → A	5
	HOMO−1 → LUMO+5	D → D	13
	HOMO → LUMO+1	D → A	7
	HOMO → LUMO+3	D → D	73
PTBF2/$PC_{71}BM$	HOMO−1 → LUMO+4	D → A	7
	HOMO−1 → LUMO+5	D → D	8
	HOMO → LUMO+2	D → A	3
	HOMO → LUMO+3	D → D	82

The absorption wavelengths and the corresponding oscillator strengths are 504.28 nm and f = 2.4924, 509.6 nm and f = 2.2431, and 631.0 nm and f = 2.7193 for the PTB7/$PC_{71}BM$, PTB1/$PC_{71}BM$, and PTBF2/$PC_{71}BM$ systems, respectively. For the molecular orbitals, see Figs. 3–5, respectively.